Comprehensive Summaries of Uppsala Dissertations
from the Faculty of Science and Technology 828

Summation-by-Parts Operators for High Order Finite Difference Methods

BY

KEN MATTSSON

ACTA UNIVERSITATIS UPSALIENSIS
UPPSALA 2003

Summation-by-Parts Operators for High Order Finite Difference Methods

Summary

Ken Mattsson

1 Introduction

In this thesis the solution of initial boundary value problems (IBVPs) are considered. We are particularly interested in time dependent wave propagating problems. Typical applications are acoustic and electromagnetic wave propagation and fluid dynamics. A recipe for solving such problems typically require proper treatment of: i) Convective and diffusive terms. ii) Boundary conditions. iii) Artificial dissipation. iv) Complex geometries.

For wave propagating problems, the computational domain is often large compared with the wavelengths, which mean that waves have to travel long distances during long times. As a result, high order accurate time marching methods, as well as high order spatially accurate schemes (at least 3rd order) are required (such as spectral elements, finite elements and finite difference methods), because of their lower phase error. Such schemes, although they are G-K-S stable [5] (convergence to the true solution as $\Delta x \to 0$), may exhibit a non-physical growth in time [1], for realistic mesh sizes. It is therefore important to device schemes which do not allow a growth in time that is not called for by the differential equation. Such schemes are called strictly (or time) stable.

In this thesis we are interested in efficient methods with a simple structure that parallelize easily on structured grids. High order finite difference methods (HOFDM) fulfill these requirements. The efficiency of high order explicit centered finite difference methods, when applied to partial differential equations, was demonstrated already by Kreiss and Oliger [14]. They determined the number of points per wavelength needed to obtain a certain phase error for semidiscrete approximations of a hyperbolic model problem with periodic boundary conditions. A calculation with a 6th order accurate method, using N grid points in each of the spatial directions, result in a phase error proportional to $(1/N)^6$. It is also shown that a 2nd order accurate method require approximately N^3 grid points in each of the spatial directions to reproduce the same phase error.

When analyzing HOFDM, the main difficulty is to show that the approximation is stable. The stability theory and boundary condition for HOFDM applied

to IBVPs [8], were until recently less developed making these codes less robust. In [12],[13] Kreiss and Scherer proved stability of difference approximations of hyperbolic IBVPs by using high order explicit difference operators satisfying a summation by parts (SBP) rule.

The main objective in this thesis have been to device stable and high order accurate finite difference schemes for hyperbolic but also for parabolic IBVPs. On complex domains our recipe to obtain such schemes is to use:

1. Accurate SBP operators.
2. Stable boundary procedures.
3. Efficient artificial dissipation.
4. Multi block structure.

The rest of the thesis will proceed as follows. In Section 1.1 we discuss some concepts and definitions. In section 1.2 the SBP properties are discussed. In section 1.3 we discuss boundary procedures. In section 1.4 the use of artificial dissipation is motivated. In section 1.5 we discuss different methodologies for solving problems on "real" geometries. In sections 2.1, 2.2, 2.3, 2.4 and 2.5 we summarize paper [I], [II], [III], [IV] and [V] respectively.

1.1 Concepts and definitions

Before we start describing the stability properties, some definitions are needed. Let the inner product for real valued functions $u, v \in L^2[a,b]$ be defined by $(u,v) = \int_a^b u\, v\, dx$ and the corresponding norm $\|u\|^2 = (u,u)$. The domain $(a \leq x \leq b)$ is discretized using N equidistant grid points,

$$x_j = a + (j-1)\, h\,, \qquad j = 1, 2..., N\,, \qquad h = \frac{b-a}{N-1}\,.$$

The numerical approximation at grid point x_j is denoted v_j, and the discrete solution vector $v^T = [v_1, v_2, \cdots, v_N]$. We define an inner product and norm for discrete real valued vector-functions $u, v \in \mathbf{R^n}$ by

$$(u,v)_H = u^T\, H\, v\,, \quad \|v\|_H^2 = v^T\, H\, v\,, \tag{1}$$

where $H = H^T > 0$.

Consider the IBVP,

$$\begin{aligned} &u_t + Pu = F(x,t) \qquad 0 \leq x \leq 1, \qquad t \geq 0 \\ &Lu(0,t) = g(t) \\ &u(x,0) = f(x)\,, \end{aligned} \tag{2}$$

where P is the differential operator, L the boundary operator, F the forcing function, f the initial data and g the boundary data. The semidiscrete approximation of (2) can be written as a system of ordinary differential equations

$$\begin{aligned} &v_t + Mv = G(t) \qquad t \geq 0 \\ &v(0) = f \ , \end{aligned} \tag{3}$$

where M is the matrix representing the spatial discretization, including the boundary conditions and G is a known vector function.

If (2) is well posed (see [8]) and $F = g = 0$ (which yield $G = 0$ in (3)), an energy estimate of the form

$$\|u\| \leq K_c e^{\alpha_c t} \|f\| \ , \tag{4}$$

exist. In (4), K_c and α_c do not depend on t. If (3) is a strictly stable difference approximation of (2), a corresponding discrete energy estimate of the form

$$\|v\|_H \leq K_d e^{\alpha_d t} \|f\|_H \ , \tag{5}$$

exist. In (5), $\alpha_d \leq \alpha_c + \mathcal{O}(h)$. This means that a strictly stable approximation has the same asymptotic time growth as the continuous problem.

The asymptotic time growth is determined by the utmost right part of the spectrum, denoted α_c and α_d in the continuous and discrete case respectively. Roughly speaking, the spectrum of the continuous problem is obtained as the singular values of the solution to the Laplace transformed version of (2) [8]. Details on how to compute the spectrum are given in [I]. The discrete spectrum are the eigenvalues of the matrix M in (3). Note that $K_c \neq K_d$ in general.

1.2 Summation-by-Parts operators

An SBP operator is essentially a centered difference scheme with a specific boundary treatment, which mimic the behavior of the corresponding continuous operator with regard to the inner product defined by (1). Consider the hyperbolic scalar equation, $u_t = u_x$. Notice first that $(u, u_t) + (u_t, u) = d/dt\|u\|^2$. Integration by parts leads to,

$$\frac{d}{dt}\|u\|^2 = (u, u_x) + (u_x, u) = u^2|_a^b \ , \tag{6}$$

where we introduce the notation $u^2|_a^b \equiv u^2(x = b) - u^2(x = a)$. Consider the semidiscrete approximation, $v_t = D_1 v$, of the hyperbolic equation. A difference operator $D_1 = H^{-1}Q$ is an SBP operator if $Q + Q^T = B$, where

$$B = diag\,(-1, 0 \ldots, 0, 1) \ , \tag{7}$$

since this leads to

$$\frac{d}{dt}\|v\|_H^2 = (v, H^{-1}Qv)_H + (H^{-1}Qv, v)_H = v^T(Q + Q^T)v = v_N^2 - v_0^2 \ . \tag{8}$$

Equation (8) is a discrete analog of the integration by parts formula (6) in the continuous case.

To handle parabolic problems we also need an SBP operator for the second derivative. Consider the heat equation, $u_t = u_{xx}$. Integration by parts leads to,

$$\frac{d}{dt}\|u\|^2 = (u, u_{xx}) + (u_{xx}, u) = 2uu_x|_a^b - 2\|u_x\|^2 \ . \tag{9}$$

The idea, on how to construct an SBP operator D_2, approximating $\partial^2/\partial x^2$, comes from studying (9). It is easy to realize that in order to fully mimic the integration by parts property we need $D_2 = H^{-1}(-D_1^T H D_1 + BS)$, where D_1 is a consistent approximation of $\partial/\partial x$, S includes an approximation of the first derivative operator at the boundary and B is given by (7). The energy method on the semidiscrete approximation, $v_t = D_2 v$ leads to,

$$\frac{d}{dt}\|v\|_H^2 = (v, D_2 v) + (D_2 v, v) = 2v_N(Sv)_N - 2v_0(Sv)_0 - 2\|D_1 v\|_H^2 \ , \tag{10}$$

a discrete analog of the integration by parts formula (9) in the continuous case.

However, it is not necessary to fully mimic the integration by parts property in order to get an energy estimate. Consider the difference operator $H^{-1}(-A + BS)$, approximating $\partial^2/\partial x^2$. The energy method leads to

$$\frac{d}{dt}\|v\|_H^2 = 2v_N(Sv)_N - 2v_0(Sv)_0 - v^T(A + A^T)v \ . \tag{11}$$

To get an energy estimate it suffice that $A + A^T \geq 0$, assuming that the boundary terms are correctly implemented.

The construction of SBP operators for the second derivative is done in paper [IV], by using the symbolic mathematics software Maple.

1.3 Boundary procedures

By using an SBP operator, a strict stable approximation for a Cauchy problem is obtained. Nevertheless, the SBP property alone does not guarantee strict stability for an IBVP, a specific boundary treatment is also required. To impose the boundary condition explicitly, i.e. to combine the difference operator and the boundary operator into a modified operator, usually destroy the SBP property. In general, this makes it impossible to obtain an energy estimate. This boundary procedure, often used in practical calculations, is referred to as the injection method and can result in an unwanted exponential growth of the solution.

The basic idea behind the Simultaneous Approximation Term (SAT) method [1] and the projection method [18],[19] is to impose the boundary conditions such that the SBP property is preserved and such that we get an energy estimate. A systematic comparison between the SAT method, the projection method, and the injection method was first done in [20], where a hyperbolic scalar equation and a hyperbolic system was considered.

In [I], a similar study was performed, considering also the linear advection-diffusion equation for which the projection method fail to be a strictly stable approximation. A similar method — a cure for the Projection method — which was introduced in [7] as a "hybrid" between the injection method and the projection method was also analyzed.

As an example of the simple, yet powerful SAT boundary procedure, we consider the hyperbolic scalar equation,

$$u_t + u_x = 0, \quad 0 \le x \le 1, \quad t \ge 0, \quad u(0,t) = g_0(t) \ . \tag{12}$$

Integration by parts leads to,

$$\frac{d}{dt}\|u\|^2 = g_0^2 - u^2(x=1) \ . \tag{13}$$

The discrete approximation of (12) using the SAT method for the boundary conditions leads to

$$v_t + H^{-1}Q\,v = -H^{-1}\tau\left\{E_0 v - e_0 g_0(t)\right\} v, \quad v(0) = f \ , \tag{14}$$

where $e_0 = [1,0,...,0]^T$ and $E_0 = diag([1,0,...,0])$. By choosing $\tau = 1$, the energy method leads to

$$\frac{d}{dt}\|v\|_H^2 = g_0^2 - v_N^2 - (v_0 - g_0)^2 \ . \tag{15}$$

Equation (15) is a discrete analog of the integration by parts formula (13) in the continuous case, where the extra term $(v_0 - g_0)^2$ introduce a small additional damping.

1.4 Artificial Dissipation

For linear hyperbolic IBVPs, stable and accurate approximations are obtained if : i) The first derivative is approximated with high order accurate SBP operators. and ii) The boundary conditions are implemented with specific boundary procedures, that preserve the SBP property, see [18], [1].

An SBP operator is essentially a centered difference scheme with a specific boundary treatment. For nonlinear convection problems it is well known that centered difference schemes require the addition of artificial dissipation to absorb the energy of the unresolved modes. This is usually accomplished by adding dissipation operators, constructed by high order undivided differences, see [17] and [4].

Consider the semidiscrete approximation

$$v_t = H^{-1}\,R\,v \quad , \ v(0) = f \ , \tag{16}$$

of a linear initial boundary value problem in one space dimension. Here we assume that the spatial operator $H^{-1}\,R$ includes the (homogenous) boundary conditions. The energy method leads to $v^T\,H\,v_t + v_t^T\,H\,v = \frac{d}{dt}\|v\|_H^2 = v^T(R + R^T)v$. Most of the relevant continuous problems have a non growing solution energy. To get a non growing solution energy also for the discrete problem, $R + R^T$ must be negative semidefinite. With the addition of an artificial dissipation term $(-H^{-1}\,S)v$ on the right hand side in (16), we get

$$v_t = H^{-1}(R - S)v \quad , \; v(0) = f \; . \tag{17}$$

A sufficient condition for stability is that the symmetric part of $(R-S)$ is negative semidefinite. However, to separate the analysis of the dissipation operator from the original problem we specifically require that

$$S + S^T \geq 0 \; . \tag{18}$$

If (16) is stable and if condition (18) hold, then (17) is stable. The remaining task is then to find S such that we obtain efficient dissipation and preserve the accuracy at the boundaries. This particular problem is addressed in [II].

1.5 Multi block structure

Generating a grid around a complex configuration is often the most time consuming aspect of the solution procedure. Constraints on the grid such as smoothness to higher order (necessary to attain design accuracy for high order methods) severely complicates the grid generation around complex configurations. This fact has limited the use of HOFDM in practical calculations to the small class of simple geometries which can be smoothly mapped onto the unit cube and led many high order practitioners to consider unstructured methods.

Examples of fully unstructured approaches are finite volume, finite element and spectral element methods. However, computational efficiency continue to make calculations on structured meshes attractive. An alternative to fully unstructured methods is the semistructured approach, in which the computational domain is broken up into a number of smooth and structured meshes in a multi block fashion. Each subdomain is discretized with a stable formulation and the blocks are patched together to a global domain by using suitable interface conditions. The main difficulty with this approach is to patch the blocks together in a stable and accurate way.

A natural way to obtain a stable and high order accurate approximation of the multi block problem, in the framework of HOFDM, is to discretize each subdomain using SBP operators and treat both the (external) boundary and (internal) interface conditions using the SAT boundary procedure. This particular approach was adopted in [2] and [15] to construct stable and conservative boundary and interface conditions for the (1D) constant coefficient Euler and Navier-Stokes equations, on multiple domains. A similar technique was used

in [11, 10, 9] for Chebyshev spectral methods. In [16] the constant coefficient analysis in [2] and [15] was extended to scalar multi-dimensional linear problems in curvilinear coordinates, including block interfaces.

In [III] and [V] numerical studies on the benefit of high order methods on complex domains were performed, considering numerical computations governed by the (2D) Euler equations on a multi block domain. Steady and transient aerodynamic calculations around an airfoil were considered, where the first derivative SBP operators and the new artificial dissipation operators developed in [II] were combined to construct high order accurate upwind schemes. The interface conditions were treated with the technique developed in [16].

2 Summary of the papers I-V

2.1 Paper I

We analyze four methods of imposing physical boundary conditions for finite difference approximations of the advection-diffusion equation (21) and of a hyperbolic system (20). The methods are: the injection method, the SAT method, the projection method and the modified projection method. To investigate numerically if the methods are strictly stable we compute the error for long time integrations, and determine the eigenvalue spectrum for the semidiscrete approximations. The semidiscrete approximations to both types of IBVPs can formally be written as

$$v_t = \begin{cases} A_P v & \text{(projection)} \\ A_S v & \text{(SAT)} \\ A_I v & \text{(injection)} \\ A_M v & \text{(modified projection)} \end{cases} , \tag{19}$$

where $A_{P,S,I,M}$ are the different matrix representations of the spatial discretization (including the homogeneous boundary conditions). The discrete spectrum are the eigenvalues to $A_{P,S,I,M}$.

The Simultaneous Approximation Term (SAT) method [1] and the projection method [18],[19] impose the boundary conditions such that the SBP property is preserved and such that we get an energy estimate. Other types of boundary procedures destroy the SBP property, which in general mean that an energy estimate cannot be obtained. In Figure, 1 the discrete spectrum for the sixth order accurate approximation of the hyperbolic system (20) are shown.

$$\begin{aligned} &u_t^{(0)} + u_x^{(0)} = 0 \qquad 0 \le x \le 1, \qquad t \ge 0 \\ &u_t^{(1)} - u_x^{(1)} = 0 \qquad 0 \le x \le 1, \qquad t \ge 0 \\ &u^{(0)}(0,t) = u^{(1)}(0,t) \quad , u^{(1)}(1,t) = u^{(0)}(1,t) \\ &u^{(0)}(x,0) = g(x) \quad , \; u^{(1)}(x,0) = h(x) \; . \end{aligned} \tag{20}$$

The continuous problem have constant energy, i.e. $\frac{d}{dt}\left(\|u^{(0)}\|^2 + \|u^{(1)}\|^2\right) = 0$, which means that the continuous eigenvalues are located on the imaginary axis.

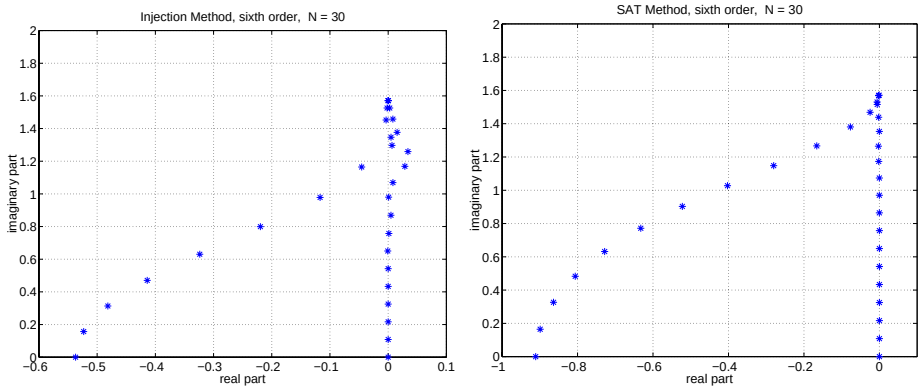

Figure 1: Discrete spectrum, sixth order case, $N = 30$.

Notice that the injection method have positive eigenvalues, which show that the 6th order approximation is unstable for this particular problem. To further investigate, numerically, if the methods were strictly stable, the l_2-error for long time integrations were computed, see Figure 2. It is clear that also the 4th order approximation using the injection method result in an unstable method.

For the hyperbolic system that we considered, the eigenvalue zero is a part of the continuous spectrum. Hence the zero eigenvalue that is always introduced by the Projection method does not destroy the growth rate. However, for problems where the largest real part of the continuous spectrum is negative, like for the advection-diffusion equation (with proper boundary conditions)

$$u_t + au_x = \epsilon u_{xx} \ , \tag{21}$$

the projection method will not result in a strictly stable approximation. This causes problem if the boundary and the initial data are inconsistent.

To examine how the solution behaves when the initial data and the boundary data do not match we compare the computation with and without inconsistent initial data at the boundaries. The error is defined as the difference between the disturbed and the undisturbed solution. The l_2 error as a function of time is presented in Figure 3, for the 6th order case, with inconsistent initial data (of magnitude 0.01) at the inflow boundary. 50 grid points are used and the solutions are advanced to time $t = 10$, using the standard 4th order Runge-Kutta method. Figure 3 show that the error introduced by the inconsistency, remain in the solution when the projection method is used.

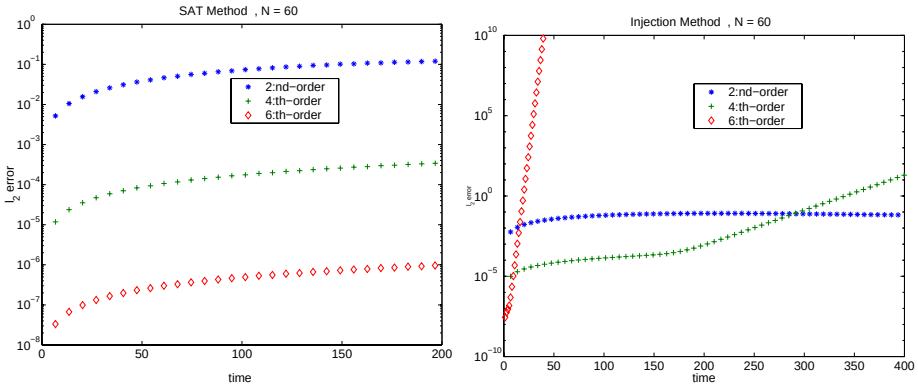

Figure 2: l_2-error as a function of t, for 2nd, 4th, 6th order case, $N = 60$. Notice the blowup in the right subfigure. The l_2-errors for the injection method are presented up to $t = 400$, to show the blowup also for the 4th order case.

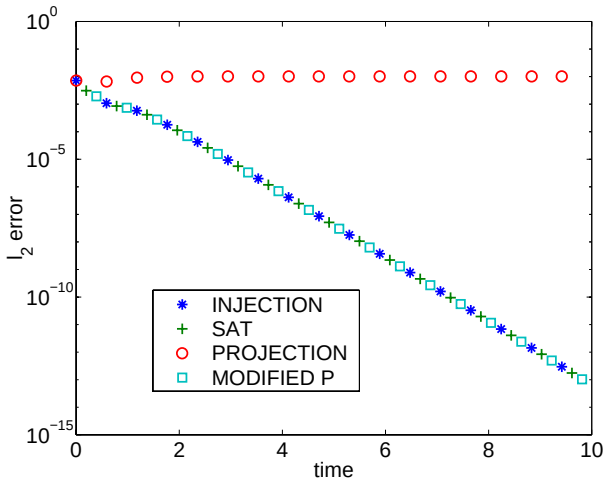

Figure 3: l_2 error as a function of time for 6th order case. Inconsistency (of magnitude 0.01) at the inflow boundary.

2.2 Paper II

To obtain efficient dissipation in the interior of the domain, the artificial dissipation operator is designed to approximate the highest possible even degree derivative within the same stencil as the base central approximation. In other words we use a centered, second order accurate undivided difference scheme of order $2\,p$ for a $(2\,p)th$ order accurate method. The main difficulty is then to modify the artificial dissipation operator at the boundaries such that accuracy and stability is preserved.

There is a variety of SBP operators approximating $\partial/\partial\,x$ to a certain accuracy, constructed with different norms H, see [12, 13, 20]. With a diagonal norm, at most pth order accuracy can be achieved at the boundary, where the internal accuracy is of order $2p$. This will result in a $(p+1)th$ order accurate approximation of the original problem. With a full norm H (the upper and lower part of the norm consist of $2\,p$ by $2\,p$ blocks), a $(2p-1)th$ order accurate boundary closure exist, which result in a $(2\,p)th$ order accurate approximation of the original problem. This is due to the fact that one can lower the accuracy by one order at a finite number of points and still obtain accuracy of order $2p$, see [6].

The form of the dissipation operator for the $(2\,p)th$ order case is given by

$$DI_{2\,p} = -\tilde{H}^{-1}\tilde{D}_p{}^T\,B_p\,\tilde{D}_p = \tilde{H}^{-1}\,S\ ,$$

where $D_p = h^{-p}\tilde{D}_p$ (the tilde sign emphasizes that there is no h dependence) is a consistent approximation of $d^p/d\,x^p$ with minimal width, $B_p + B_p^T \geq 0$, and H is the $(2\,p)th$ order norm. This clearly leads to stability, see (18). The main result, shown in this paper, is that in order to preserve accuracy at the boundaries in the full norm case, B_p must depend on the number of grid points. To obtain minimal width and accuracy of order $2\,p$ in the interior, B_p must be a diagonal matrix that approximate a smooth function. Without restriction we choose B_p to be diagonal also at the boundaries. To obtain the desired accuracy also at the boundaries (in the full norm case), we required the diagonal of B_p to be the restriction onto the grid of a piecewise smooth function, that increase from a low (proportional to $\mathcal{O}(h^{p-1})$) up to a higher constant level, over a *fixed* portion of the domain, such that derivatives up to order $p-2$ vanish at the boundaries and at the transition points (see Figure 4).

In [17] a symmetric and negative semidefinite dissipation operator, $DI_e = -\tilde{D}_4{}^T\,B_e\,\tilde{D}_4$ is presented, where $B_e = diag(0,0,1,\cdots,1,0,0)$. This operator is suitable for a 5th order accurate method since the interior scheme is of order 8 and 4th order accurate at the boundaries. However, using this operator as artificial dissipation for the 8th order diagonal norm case (which is globally of order 5) will not result in an energy estimate. A modification that leads to an energy estimate would be to multiply DI_e with the inverse of the norm, i.e. to let $DI_8 = \tilde{H}^{-1}DI_e$. In Figure 5, the l_2-error for long time integrations are

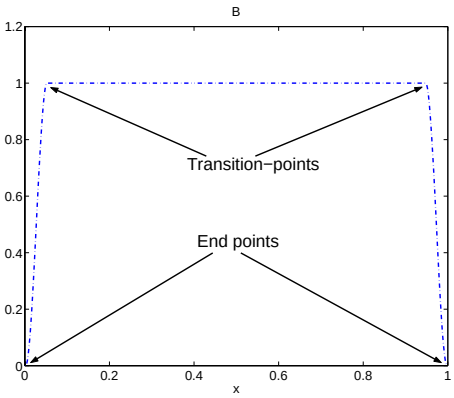

Figure 4: Example of B_p in the 6th order case. In the transition region, which occupy five percent of the total region, we use a 3rd order polynomial that increase from h^2 to one, such that the first derivative is zero at the transition points and at the boundaries (end points).

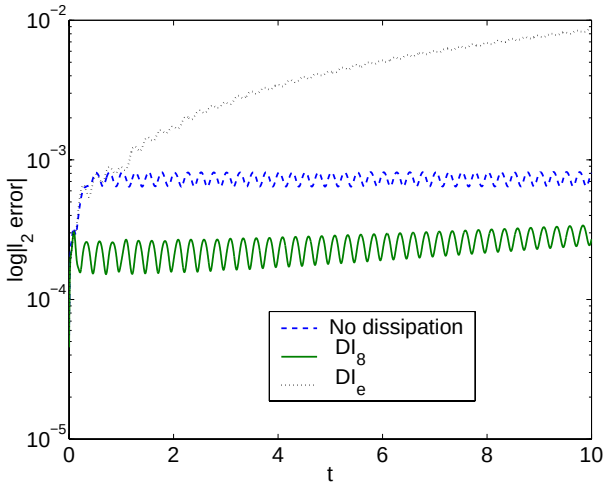

Figure 5: Problem (20), l_2-error as a function of t with DI_e, DI_8 as dissipation. $N = 50$. Also included is the case with no dissipation.

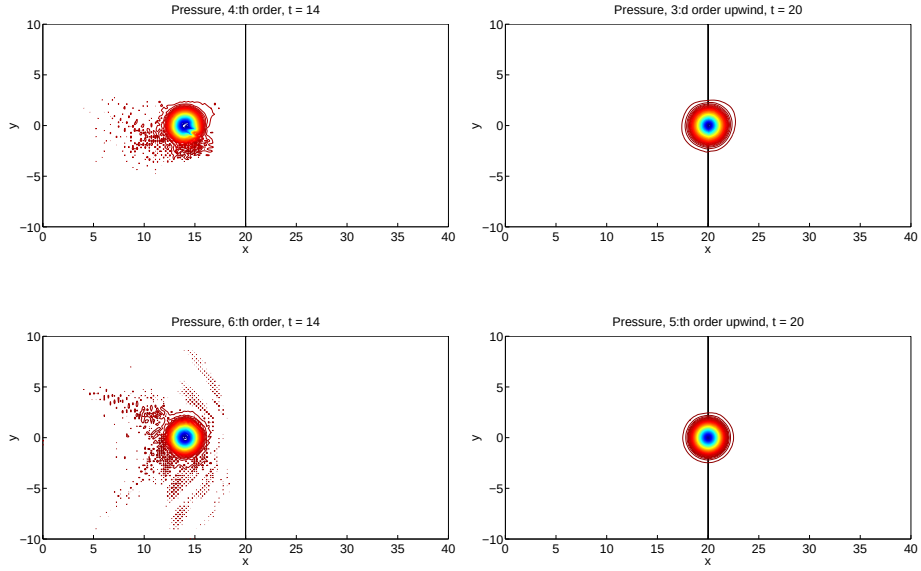

Figure 6: Pressure contour. Comparing the stability properties for a truly nonlinear problem, with (left subfigures) and without (right subfigures) the addition of artificial dissipation.

shown, where the hyperbolic system (20) is considered. Clearly the use of DI_e as dissipation for the 8th order diagonal norm case result in an unstable method for this problem (due to positive eigenvalues in the discrete spectrum).

To test the dissipation operators in a more realistic setting, we considered the numerical computation of solutions governed by the 2-D Euler equations. The new dissipation operators were combined with the first derivative SBP operators to obtain 3rd and 5th order accurate upwind schemes. Figure 6 show the computation of a vortex convected through an empty domain with and without the addition of artificial dissipation. The calculations (4th and 6th order accurate) using non-dissipative schemes are stopped a short moment before calculation of the vortex breaks down at $x = 14$, due to non linear instability. The calculations using the dissipative upwind schemes propagate the vortex without any problem, even after reaching the internal boundary at $x = 20$.

2.3 Paper III

A numerical study on the benefit of high order methods for transient aerodynamics is performed. The first derivative SBP operators and the new artificial dissipation operators derived in [II] were combined to construct 3rd and 5th or-

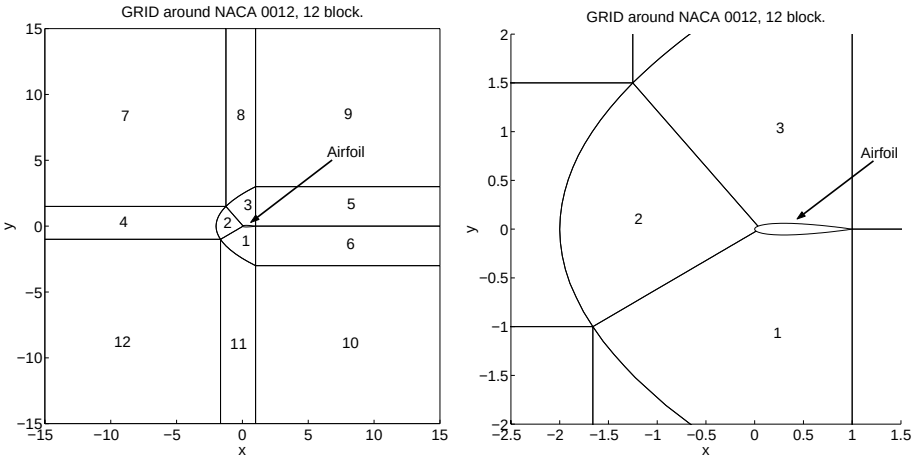

Figure 7: The computational domain, divided into 12 blocks, around a NACA0012 airfoil. The right subfigure is a close up.

der accurate upwind schemes, which were used to compute solutions to a vortex-airfoil interaction, governed by the Euler equations. For the sake of comparison, computations are also done using a 2nd order central scheme with a 4th order difference as artificial dissipation, scaled as in the 3rd order upwind case.

To obtain a suitable grid for computing the vortex-airfoil interaction, the computational domain was split into 12 blocks (see Figure 7). To maintain stability in the multi block setting, the interface conditions were treated with the SAT method [16]. The computations run in parallel and each block was handled by a single processor. There are other, more general choices. For instance we could let processors handle more than one block, or (and) we could let several processors work together on a single block. With our choice each processor only has to communicate with the other processors through the block interfaces. This particular methodology makes the problem particularly easy to parallelize. To obtain efficiency it is crucial that the number of grid points in each block is approximately the same (to obtain load balance). Numerical calculations were performed on a sequence of successively finer meshes (here denoted: coarse, fine and finest). The number of grid points on successively finer meshes are doubled in each direction.

To validate the quality of the solver we compared the steady solution of Mach number 0.63 around a NACA0012 airfoil of 2 degree angle of attack with the result obtained using a node centered finite volume solver (EDGE [3]). The results agreed well.

We are interested in computing the interaction of a vortex hitting an airfoil.

As initial data we used steady solutions and introduced the vortex as boundary data on the left boundary, see Figure 7. The vortex is swept downstream towards the airfoil and eventually hits it, see Figure 8. The 2nd order method, although it gives reasonable result for the integrated properties such as lift, gives a completely different solution compared to the 3rd and 5th order upwind methods on the fine grid. This shows that a reasonable agreement in the integrated properties does not necessarily imply good agreement of the fine structures in the flowfield.

Summing up, numerical results show that the multi block code run efficiently on a parallel computer. The computations of the vortex-airfoil interaction showed, that for time dependent problems and fine structures, high order methods are necessary to accurately compute the solution, on reasonable fine grids.

2.4 Paper IV

In [IV] finite difference approximations of second derivatives, which satisfy a summation by parts rule were derived for the 4th, 6th and 8th order case based on both the full and the diagonal norms, by using the symbolic mathematics software Maple. For linear initial boundary value problems, strictly stable and accurate approximations are obtained (shown in [I]) if :

- The derivatives are approximated with accurate SBP operators.
- The proper boundary conditions are implemented with the SAT method.

High order accurate SBP operators for the first derivative were first developed in [12, 13] and later in [20]. To facilitate the construction of highly accurate and stable approximations of mixed hyperbolic-parabolic problems, high order accurate SBP operators also for the second derivative are needed. To obtain stability it is necessary that the second derivative approximation is based on the same norm as the SBP operator approximating the first derivative.

The error analysis performed in this paper indicated that the second derivative approximation could be closed at the boundaries with approximations two orders less accurate, compared to the design order of the scheme, and still maintain the internal accuracy. The error analysis require that the numerical approximation results in an energy estimate. In order to verify the accuracy requirements, two types of second derivative approximations were derived (in the full norm case) for each order of accuracy. The first approximation was closed at the boundaries with stencils two orders less accurate, compared to the internal accuracy. The second type was closed with one order less accurate approximations at the boundaries, compared to the internal accuracy.

A convergence study for the semidiscrete approximation of the advection-diffusion equation (21) was done. Table 1 show the result for the 4th order case (full norm) where the first derivative approximation is treated with 3rd order

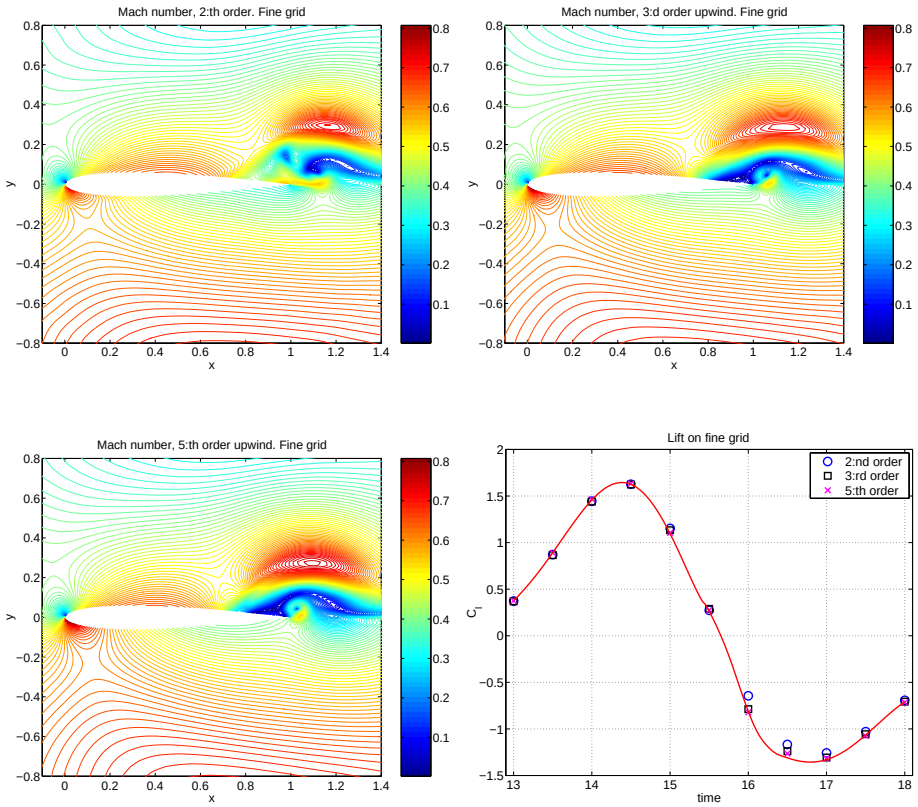

Figure 8: Vortex hitting a NACA0012 at x=1. Comparing 3rd and 5th order upwind to a second order method. Notice the similarity in the flowfields for the 3rd and 5th order methods. The down-right subfigure show the lift at different times for the same grid as the other subfigures. The solid line is the 3rd order reference solution on a finer grid.

N	l_2	q	l_2^v	q^v
40	-4.31		-3.11	
60	-5.06	4.14	-3.67	3.11
100	-5.98	4.09	-4.36	3.08
200	-7.20	4.04	-5.28	3.04
300	-7.91	4.02	-5.82	3.03

N	l_2	q	l_2^v	q^v
40	-4.24		-3.84	
60	-4.97	4.09	-4.58	4.09
100	-5.89	4.06	-5.48	4.02
200	-7.11	4.04	-6.69	3.98
300	-7.82	4.02	-7.39	3.98

Table 1: $log(l_2 - error)$ and convergence rate for the 4th order case, based on the block norm. The left table: with 2nd order boundary closure. The right table: 3rd order boundary closure. In the computations marked v the stability conditions are violated by improper choice of penalty parameters. Notice the loss of convergence, in the left table.

accurate boundary closures. Two types of second derivative approximations was tested. The first approximation is closed at the boundaries with stencils of order 2. The second type is closed at the boundaries with stencils 3rd order accurate. We have included also the case where the stability conditions are violated by an improper choice of penalty parameters, which means that the energy estimate no longer holds. By violating the stability conditions we obtain a 3rd order accurate approximation if the second derivative approximation is closed at the boundaries with 2nd order stencils. A convergence study for a hyperbolic problem ($\epsilon = 0$ in (21)) was also performed. The result showed, in agreement with [6], that in order to preserve the internal accuracy of the scheme we must close the boundaries with at most one order less accurate stencils.

This motivated the investigation of an incompletely parabolic system, i.e. a model of the compressible Navier-Stokes equations. We considered

$$u_t + Cu_x = Du_{xx} \ , \tag{22}$$

where

$$u = \begin{bmatrix} u^{(1)} \\ u^{(2)} \end{bmatrix}, \quad C = \begin{bmatrix} 1 & 1 \\ 1 & -1 \end{bmatrix}, \quad D = \begin{bmatrix} 0 & 0 \\ 0 & \epsilon \end{bmatrix} \ , \epsilon > 0 \quad .$$

The energy method was used to derive suitable boundary conditions.

The convergence study showed that a difference approximation, with boundary closures two orders less accurate for the approximation of the second derivative, and a physical boundary condition one order less accurate, compared to the internal accuracy, maintain the design order of accuracy. If the stability condition is violated, the overall convergence rate is again reduced by one order. Table 2 show the result for the 6th order full norm case.

In order to test the second derivative SBP operators in a more realistic setting, we considered the numerical computation of the flow around a NACA0012 airfoil, governed by the 2-D Navier-Stokes equations, where the pure second

N	l_2	q	l_2^v	q^v
30	-4.75		-4.57	
60	-6.66	6.20	-6.05	4.79
90	-7.72	5.94	-6.92	4.91
120	-8.48	6.01	-7.55	4.96
150	-9.07	6.00	-8.03	4.95

N	l_2	q	l_2^v	q^v
30	-4.76		-4.72	
60	-6.66	6.16	-6.72	6.48
90	-7.72	5.93	-7.79	6.03
120	-8.48	6.02	-8.55	5.97
150	-9.07	6.05	-9.13	5.98

Table 2: $log(l_2 - error)$ and convergence rate in the 6th order case, based on the block norm. The left table: 4th order boundary closure. The right table: 5th order boundary closure. In the computations marked v the stability conditions are violated by improper choice of penalty parameters. Notice the loss of convergence, in the left table.

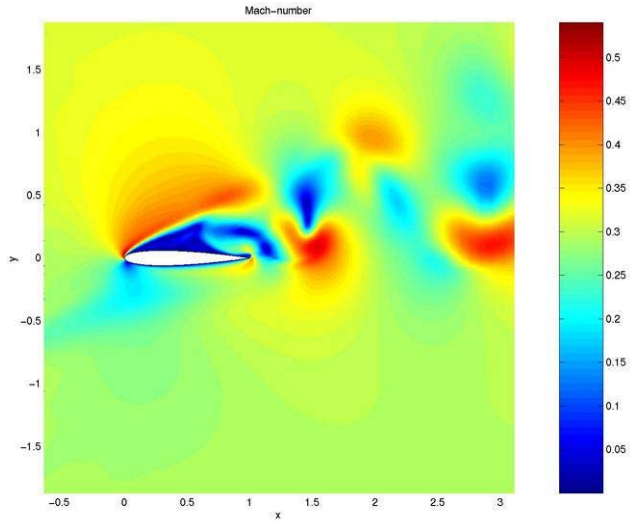

Figure 9: Navier-Stokes solution around a NACA0012 airfoil at Mach number 0.3 at 20 degree angle of attack, using a 3rd upwind method, and a Reynolds number of 10000.

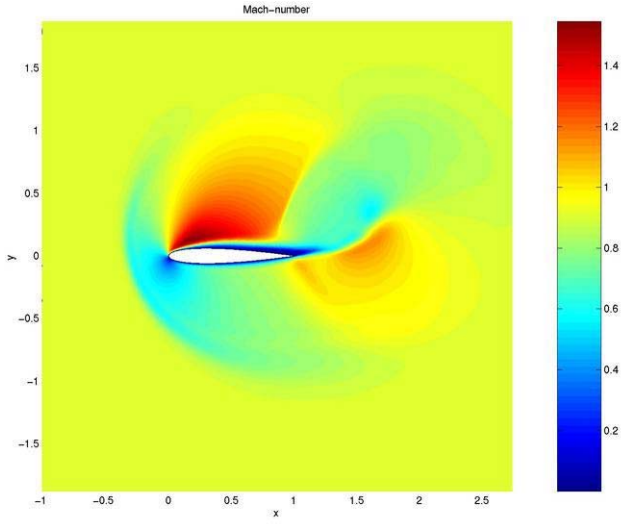

Figure 10: Navier-Stokes solution around a NACA0012 airfoil at Mach number 0.9 at 20 degree angle of attack, using a 3rd upwind method, and a Reynolds number of 10000.

derivative terms were approximated with the newly derived SBP operators, see Figures 9, 10.

Summing up, numerical tests indicate that there is a close connection between the overall convergence rate and the stability estimate. If the stability conditions are violated, such that the energy estimate no longer holds, the overall convergence rate is reduced by one order by using a second derivative approximation with two order lower accuracy at the boundaries, compared to the internal accuracy of the scheme. The numerical results also show that the new second derivative SBP operators work well in realistic applications.

2.5 Paper V

In this paper energy stability for HOFDM on curvilinear grids and its impact on steady state calculations were considered. To accurately compute fine structures for time dependent problems, high order methods are necessary, as concluded in [III]. Such problems often require good steady state solutions as initial data and in this paper we addressed some issues related to the computation of steady state solutions on complex domains. By using SBP operators combined with the SAT boundary procedure, stable schemes are obtained for IBVPs on Cartesian grids. In [21] it is shown that stability is destroyed when SBP operator based

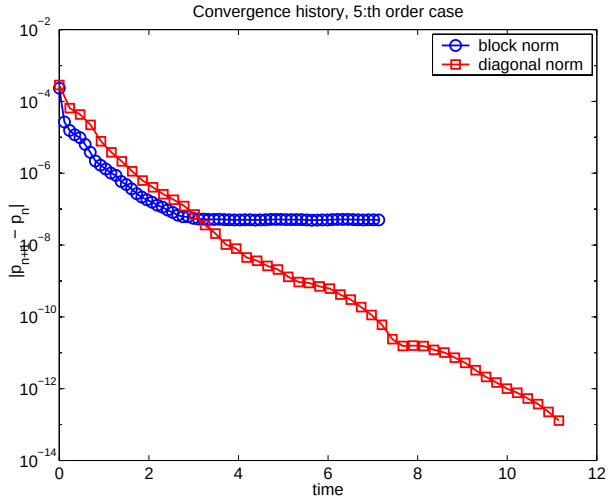

Figure 11: Steady state convergence, comparing the 5th order upwind schemes, based on the 8th order diagonal and the 6th order block norm respectively.

on block norms are used in schemes applied on curvilinear grids. However, stability is recovered if SBP operator based on diagonal norms are used. The major disadvantage with the diagonal norm schemes is the loss of accuracy at the boundaries. A scheme based on a $2p\,th$ order diagonal norm is only pth order accurate at the boundaries, which globally results in a scheme of order $p+1$. Thus, the internal scheme is unnecessary accurate and wide. However, the loss of efficiency is truly marginal if upwind methods are used.

The first derivative SBP operators and the new artificial dissipation operators derived in [II] were combined to construct a 5th order accurate upwind scheme based on the 8th order diagonal norm. As a test case we considered the steady solution around a NACA0012 airfoil at 2 degrees angle of attack and Mach-number (Ma) 0.63, governed by the Euler equations. As a comparison, also a 5th order accurate upwind scheme based on the 6th order block norm was constructed. The convergence history for both schemes, are shown in Figure 11, where it can be seen that only the scheme using diagonal norm converge. The solution is considered to have reached steady state when the residual is less than 10^{-12}.

In [20] analytical expressions for the first derivative SBP operators of different orders are derived. These operators contain free parameters to be chosen. In [20] they are chosen to give the minimal width of the operator near the boundary. However, in order to speed up convergence to steady state it is essential that the spectral radius of the numerical scheme is minimal. In particular when explicit time stepping is performed. In Appendix A in [20] the

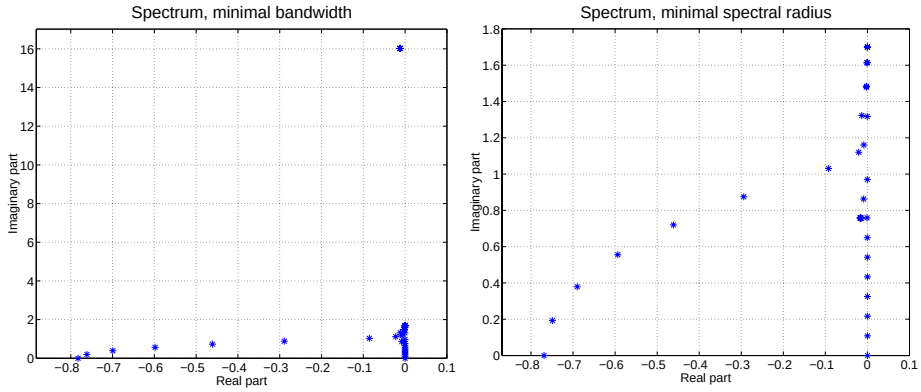

Figure 12: Discrete spectrums for the schemes based on the diagonal 8th order norm. Note the large imaginary value for the non-optimal case, in the left subfigure.

parameters x_1, x_2 and x_3 for the 8th order diagonal norm operator was chosen, $x_1 = 1714837/4354560$, $x_2 = -1022551/30481920$, $x_3 = 6445687/8709120$, to obtain a minimal bandwidth. Our parameter search led to, $x_1 = 0.649$, $x_2 = -0.104$, $x_3 = 0.755$, and a much smaller spectral radius was obtained. The term spectrally optimized is used below to denote the new operator with reduced spectral radius.

To demonstrate the efficiency we considered the hyperbolic system (20) discretized using the spectrally and non-spectrally optimized operators. In Figure 12 the discrete spectrums are shown. The spectral radii differs by a factor approximately 9.4 in favor of the operator with reduced spectral radius. Furthermore, the largest possible quotient $CFL = \Delta t/\Delta x$ was deduced experimentally and found to be $CFL_{opt} = 1.65$ and $CFL_{nonopt} = 0.176$ (also approximately a factor 9.4). Of course, as dissipation is added to the operator to make it upwind, the spectrum is altered. But it only seems to give a small perturbation of the spectrum and CFL number. Also in the airfoil computations the timestep could be increased approximately a factor 9 by using the spectrally optimized SBP operator.

To test the accuracy obtained in the airfoil calculations, numerical calculations were performed on a sequence of successively finer meshes. For the sake of comparison, computations were also done using a 2nd order central scheme with a 4th order difference as artificial dissipation. The l_2-errors of the Mach-number for the coarser grids are displayed in Table 3. Table 3 show that the errors are less in the 5th order case. However the convergence rate is about 2 in both cases. The non-optimal convergence rate of the fifth order method is probably due to a

$grid$	$2nd$	$5th$
1	0.0208	0.0135
2	0.0058	0.0033

Table 3: Steady state solution around NACA0012, $Ma = 0.63$, 2 degrees angle of attack. The l_2-errors of the Mach-number for different grids and order of accuracy.

blend of different reasons. The grid, obtained with a standard commercial grid generator with an elliptical smoother, is probably noon-smooth as indicated by a bad grid quality index (a measure comparing finite differences of the grid points at different orders of accuracy.). Further, there are density oscillations in front of the airfoil. These oscillations are reduced as the grid is refined. Similar oscillations are also seen in the second order scheme. The reason for these oscillations are probably due to lack of artificial dissipation perpendicular to the symmetry line in the flow solution.

Summing up, the numerical results showed that energy stability is important when computing steady state solutions to IBVPs. This led us to consider SBP diagonal norm schemes, where stability proofs using the energy method are obtainable. Furthermore, we improved the difference operator such that a considerably larger time step could be used, which led to fast convergence to steady state. The computations indicated that lack of numerical dissipation as well as bad grid quality may destroy the convergence rate for high order of accuracy.

References

[1] Mark H. Carpenter, David Gottlieb, and Saul Abarbanel. The stability of numerical boundary treatments for compact high–order finite–difference schemes. *J. Comput. Phys.*, 108(2), 1994.

[2] Mark H. Carpenter, Jan Nordström, and David Gottlieb. A stable and conservative interface treatment of arbitrary spatial accuracy. *J. Comput. Phys.*, 148, 1999.

[3] Peter Eliasson. A Navier-Stokes solver for unstructured grids. Scientific report FOI-R–0298–SE, The Swedish Defense Research Agency, Stockholm, 2001.

[4] L.-E. Eriksson. Boundary conditions for artificial dissipation operators. Technical Report FFA TN 1984-53, The Aeronautical Research Institute of Sweden, Aerodynamics Department, Stockholm, Sweden, 1984.

[5] B. Gustafsson, H. O. Kreiss, and A. Sundström. Stability theory of difference approximations for mixed initial boundary value problems. *Math. Comp.*, 26(119), 1972.

[6] Bertil Gustafsson. The convergence rate for differnce approximations to general mixed initial boundary value problems. *SIAM J. Numerical Analysis*, 18(2):179–190, 1981.

[7] Bertil Gustafsson. On the implementation of boundary conditions for the methods of lines. *BIT*, 38(2), 1998.

[8] Bertil Gustafsson, Heinz-Otto Kreiss, and Joseph Oliger. *Time dependent problems and difference methods.* Wiley, New York, 1995.

[9] J. S. Hesthaven. A stable penalty method for the compressible Navier–Stokes equations: II. one-dimensional domain decomposition schemes. *SIAM J. Sci. Comput.*, 18:658, 1997.

[10] J. S. Hesthaven and D. Gottlieb. A stable penalty method for the compressible Navier–Stokes equations: I. open boundary conditions. *SIAM J. Sci. Comput.*, 17:579, 1996.

[11] D. A. Kopriva. Spectral methods for the Euler equations, the blunt body problem revisited. *AIAA Paper*, 29:1458, 1991.

[12] H.-O. Kreiss and G. Scherer. Finite element and finite difference methods for hyperbolic partial differential equations. *Mathematical Aspects of Finite Elements in Partial Differential Equations., Academic Press, Inc.*, 1974.

[13] H.-O. Kreiss and G. Scherer. On the existence of energy estimates for difference approximations for hyperbolic systems. Technical report, Dept. of Scientific Computing, Uppsala University, 1977.

[14] Heinz-Otto Kreiss and Joseph Oliger. Comparison of accurate methods for the integration of hyperbolic equations. *Tellus XXIV*, 3, 1972.

[15] Jan Nordström and Mark H. Carpenter. Boundary and interface conditions for high order finite difference methods applied to the Euler and Navier–Stokes equations. *J. Comput. Phys.*, 148, 1999.

[16] Jan Nordström and Mark H. Carpenter. High-order finite difference methods, multidimensional linear problems and curvilinear coordinates. *J. Comput. Phys.*, 173, 2001.

[17] Pelle Olsson. *The Numerical Behavior of Stable High-Order Finite Diffrence Methods.* PhD thesis, Uppsala University, Dep. of Scientific Computing, Uppsala Univ., Uppsala, Sweden, 1992.

[18] Pelle Olsson. Summation by parts, projections, and stability I. *Math. Comp.*, 64:1035, 1995.

[19] Pelle Olsson. Summation by parts, projections, and stability II. *Math. Comp.*, 64:1473, 1995.

[20] Bo Strand. *High–Order difference approximations for hyperbolic initial boundary value problems.* PhD thesis, Uppsala University, Dep. of Scientific Computing, Uppsala Univ., Uppsala, Sweden, 1996.

[21] Magnus Svärd. On coordinate transformation for summation-by-parts operators. *Journal of Scientific Computing*, 18, 2003.